Nanoscale

Accepted Manuscript

This article can be cited before page numbers have been issued, to do this please use: M. ewald, S. henry, E. Lambert, C. Feuillie, C. Bobo, C. Cullin, S. Lecomte and M. Molinari, *Nanoscale*, 2019, DOI: 10.1039/C8NR08714H.

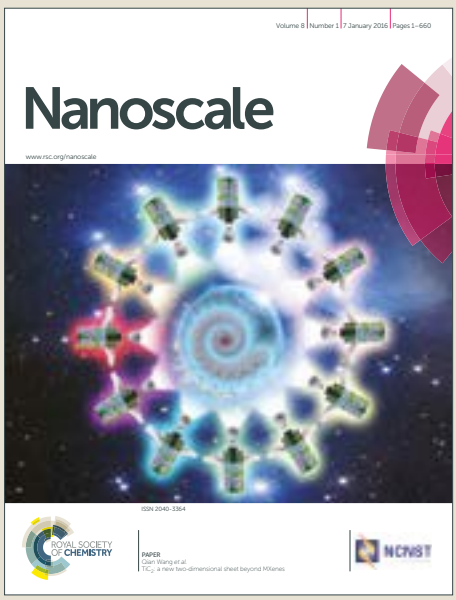

ROYAL SOCIETY OF CHEMISTRY

rsc.li/nanoscale

View Article Online
DOI: 10.1039/C8NR08714H

Nanoscale

ARTICLE

High speed atomic force microscopy to investigate the interactions between toxic $A\beta_{1\text{-}42}$ peptides and model membranes in real time: impact of the membrane composition

Received 00th January 20xx,
Accepted 00th January 20xx

DOI: 10.1039/x0xx00000x

www.rsc.org/

M. Ewald[a,+], S. Henry[b,+], E. Lambert[a], C. Feuillie[b], C. Bobo[b], C. Cullin[b], S. Lecomte[b,*], M. Molinari[a,b,*]

Due to an aging population, neurodegenerative diseases have become a major health issue, the most common being Alzheimer's disease. The mechanisms leading to neuronal loss still remain unclear but recent studies suggest that soluble Aβ oligomers have deleterious effects on neuronal membranes. Here, high-speed atomic force microscopy was used to assess the effect of oligomeric species of a variant of $A\beta_{1\text{-}42}$ amyloid peptide on model membranes with various lipid compositions. Results showed that the peptide does not interact with membranes composed of phosphatidylcholine and sphingomyelin. Ganglioside GM1, but not cholesterol, is required for the peptide to interact with the membrane. Interestingly, when they are both present, a fast disruption of the membrane was observed. It suggests that the presence of ganglioside GM1 and cholesterol in membranes promotes the interaction of the oligomeric $A\beta_{1\text{-}42}$ peptide with the membrane. This interaction leads to the membrane's destruction in a few seconds. This study highlights the power of high-speed atomic force microscopy to explore lipid-protein interactions with high spatio-temporal resolution.

Key words: Atomic Force Microscopy, high-speed AFM, nanoscale characterization, amyloid peptide, toxic oligomers, model membrane, membrane composition

Introduction

Alzheimer's disease (AD) is the most common neurodegenerative disease leading to 70% of dementia cases. AD belongs to amyloidopathies, and is characterized by the presence of neurofibrillary tangles and amyloid plaques in the patient's brain. These tangles and plaques are formed by protein (or peptide) misfolding, which self-assemble into amyloid fibers. Despite intense research in the field, the pathogenic events leading to neurodegeneration in AD remain elusive. It is particularly unclear which mechanisms are directly or indirectly responsible for neuronal death. Various hypotheses have been proposed over the years and are still being investigated. The major one is called the amyloid cascade hypothesis and is based on the major role of *Aβ* amyloid plaques in cell death and dementia.

However, it is now widely admitted that the disorder commencement is not directly correlated to the presence of amyloid plaques or fibers, but more likely due to the formation of intermediate species and to their interaction with membranes. Even if such intermediates are not yet fully characterized, soluble Aβ oligomers are believed to be the toxic species interacting with cell membranes leading to their disruption and cell death. Several mechanisms have been suggested to describe such interactions and are referenced as follows: covering of the membrane (carpet effect), permeation of the membrane (pore formation), and membrane dissolution (detergent effect)[1]. These mechanisms seem to be strongly affected by the lipid composition of the membranes. As a consequence, depending on their composition[2], the interaction of the peptide with the membrane could lead to the membrane's destruction. The parameters such as composition, charge and organization of membrane lipids will confer special features in the interaction mechanisms[3-7]. From past studies, cholesterol and gangliosides appeared to play a crucial role in the interaction of $A\beta_{1\text{-}42}$ with lipid membranes although their specific functionality remains unclear in these processes[8-10]. Cholesterol

[a] LRN EA 4682, Université de Reims Champagne-Ardenne, F-51685 Reims, France.
[b] CBMN, CNRS UMR 5248, IPB, Université de Bordeaux, 33607 Pessac, France.
[+] the authors have equally contributed to this work
* Corresponding authors: michael.molinari@u-bordeaux.fr, s.lecomte@cbmn.u-bordeaux.fr
Electronic Supplementary Information (ESI) available: [details of any supplementary information available should be included here]. See DOI: 10.1039/x0xx00000x

View Article Online
DOI: 10.1039/C8NR08714H

and ganglioside GM1 are two essential components of cell membranes playing important role for development, proliferation, differentiation and maintenance of neuronal tissues and cells. Both together, they are able to form characteristic lipid microdomains that act as a target for the peptides[1,11-15]. Among all the different lipids present in neuronal membranes, ganglioside GM1 would have the higher affinity for Aβ in this process[16].

Interaction between Aβ and membranes is a complex issue to address because of the numbers of parameters to take into account. Indeed, not only the lipid composition influence the result but also the origin of Aβ[17] or their aggregation state during experiments (monomers, oligomers, protofibrils or fibrils). In this study, $A\beta_{1\text{-}42}$ amyloid peptide was obtained in vivo using an alternative procedure[18,19] to produce highly pure $A\beta_{1\text{-}42}$. A genetic screening in yeast allowed to isolate mutants generated by mutagenesis of the $A\beta_{1\text{-}42}$ peptide. The toxicity of the different mutants were assessed in yeast, and one highly toxic mutant, compared to the wild type, was selected. This mutant presented a single mutation consisting in replacing a G residue by a C residue in position 37. The resulting mutant oligomers (oG37C) have a high tendency to form oligomers in vitro but are stable in solution. It consists of ten monomers and it is characterized by a secondary structure in antiparallel beta-sheets. It was chosen because of its higher toxicity in yeast and its oligomeric stable state[20] that does not undergo fibrillation. Thus, only the interaction between oligomers and lipid bilayers could be estimated without the interference of any other intermediate species of Aβ.

To fully understand the mechanisms of interaction between oG37C and model membranes, it is necessary to get data at the biomolecular scale to better understand the dynamic of such processes. Past studies of interactions between lipid systems and Aβ encompass conventional techniques such as fluorescence[21], electron microscopy[22], confocal microscopy[23], vibrational microscopy[24] and atomic force microscopy[25,26]. Nevertheless, these methods are either limited by a low spatial or low temporal resolution.

In this work, high-speed atomic force microscopy (HS-AFM) was used to follow the dynamic interaction between Aβ peptide variant and model membranes at the molecular scale. This technique is particularly suitable to overcome dynamics limitation while keeping a high spatial resolution. Indeed, it gives access to dynamic data at a biomolecular scale[27] thanks to its sub-second time acquisition and its high lateral resolution. Thus, HS-AFM is a perfect imaging tool to identify the dynamics of the interaction mechanisms and to better understand the importance and the role of ganglioside GM1 and cholesterol in the interaction between $A\beta_{1\text{-}42}$ and model membranes. Lipid compositions were selected in order to get relevant models. Starting from a simple model of 1-Palmitoyl-2-oleoylphosphatidylcholine (POPC) and sphingomyelin (SM), either cholesterol (Chol) or ganglioside GM1 or both of them, were then added to assess the importance of each component in the interaction process. The interaction with the oligomer oG37C was first investigated using simple model of phosphatidylcholine and sphingomyelin (SM/PC). This lipid model was then enriched with either cholesterol, ganglioside GM1 or both. The HS-AFM results showed that according to the composition of the membranes, distinct mechanisms are involved in the interaction with the toxic amyloid peptide. Real-time experiments demonstrated that a cooperation between cholesterol and GM1 is necessary to obtain a detergent effect of oG37C on the membranes leading to their disruption in a few seconds. This study highlights the power of HS-AFM to explore lipid/protein interactions with high spatio-temporal resolution.

Results and discussion

$A\beta_{1-42}$ oG37C and membrane morphologies

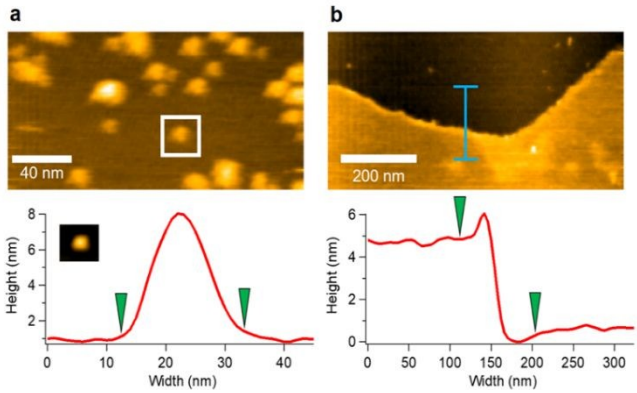

Figure 1: HS-AFM image of toxic amyloid peptide $A\beta_{1-42}$ oG37c characterization (a) and of lipid bilayer (b). Extracted picture in Fig.1a has the following characteristics: scan area, 200 × 100 nm² with 150 × 75 pixels². The white square box on Fig.1a refers to the magnified biomolecule displayed below with its section profile. The peptide has a diameter of 17.8 nm and a height of 9.6 nm. Fig. 1b reveals the interface between the mica substrate and a lipid bilayer, here made of SM/POPC/Chol/GM1 and the blue line indicates the localization of the cross section displayed below. Its scan area is 800 × 800 nm² with 200 × 200 pixels². The height of the membrane around 5 nm corresponds to a lipid bilayer.

On Figure 1a, a representative image of $A\beta_{1\text{-}42}$ oG37C oligomers deposited on a mica substrate has been extracted from the ESI3 video. Most of the oligomers are isolated with a spherical shape even if some aggregates of 2 or 3 oligomers are sometimes observed after diffusion on the substrate. The isolated oligomer selected on the image is around 17.8nm wide and 9.6nm height as observed elsewhere[28]. Statistical analysis performed on around 300 oligomers (see ESI1), the size (between 10 and 30nm) and height (between 6 and 16nm) distributions are

View Article Online
DOI: 10.1039/C8NR08714H

homogeneous with an average diameter around 20 nm and a height around 10 nm. This is in agreement with the size of 7 to 15 monomers of $A\beta_{1-42}$[29]. Additionaly, the interest of using this peptide mutant is that it does not form fibrils or change its structure with time as it is shown in ESI 1 (c) and (d). Even after incubation in the conditions used for the other experiments of the paper, it is seen that they remain in their oligomeric form. No self-assembly process was observed. This is important for this study as it enables to clearly focus on the membrane composition impact by avoiding any effects that could come from the peptide structure evolution with time. This confirms that only the oligomeric form of Aβ will interact with lipid bilayers during the HS-AFM experiments. We can therefore guarantee that only oligomeric forms will be responsible for the peptide-membrane interaction recorded during experiments. Regarding their diffusion on the bare substrate, two populations could be evidenced with some peptides that seem stuck on the mica while others are moving on the substrate. Diffusion coefficient values of around 38 nm²/s were calculated. The diffusion coefficients of 38 nm^2/s for our oligomers on mica or on membranes would be consistent with slow diffusing proteins as observed in other studies[30-32] even if peptides could also diffuse at a rate faster than the setup capabilities.

As for the lipid layers, the experiments were systematically performed on an area where the mica substrate and the membrane could be observed simultaneously. Thus, for each image, it was possible to check the thickness of the membrane to ensure that the deposition was correctly made. In Fig. 1b, a typical AFM image of a model membrane is observed with a thickness of around 5/6 nm corresponding to a single bilayer. For each condition, similar thicknesses were observed with some minor variation as a function of the membrane composition even if from time to time, two to three bilayers (but never more) could be observed.

Interaction between $A\beta_{1-42}$ oG37C and SM/POPC bilayer

The interactions between the toxic oG37C peptide and a model membrane composed in a first step of sphyngomyelin and phosphatidylcholine (SM/POPC, 20/80) was investigated. HS-AFM images extracted from recorded video (see video ESI2) are shown in Figure 2.

After the vesicle fusion on the substrate, a region of interest that exhibits both membrane and mica surfaces was selected. Following the injection of the toxic peptide oG37C at t = 18s, the peptide started to accumulate around the membrane and in the cavities. No interaction between the peptide and the membrane seem to occur. The peptide was mainly localized on the mica around the membrane and seemed to be anchored on the substrate. After around 5 minutes, the physical integrity of the membrane remained unchanged while the accumulation of the oligomers on the substrate was evident so as the absence of peptides on the membrane even a long time after the injection. On the video, a small drift of the image and a loss of the imaging details of the membrane surface due to a change in the z-scale are observed as we have to change the feedback imaging parameters in real-time to counterbalance the oligomer motion in the solution and on the substrate. Also, after the injection, one can notice some minor changes with time regarding the surface of the membranes (for instance around 60s and 110s) which could be due to lipid remodeling upon peptide addition[33] or could also be consecutive to a lateral compression stress induced by the "packing" of peptides on the mica close to the membrane patches[34]. However, the overall shape of the lipid membrane in figure 2 does not change after addition of the peptide, and the area covered by the membrane is not reduced, supporting our claim that the oligomers weakly interact with SM/DOPC membranes or with diffusion at speed faster than the imaging speed.

View Article Online
DOI: 10.1039/C8NR08714H

Interaction between $A\beta_{1-42}$ oG37C and SM/POPC/Chol bilayer

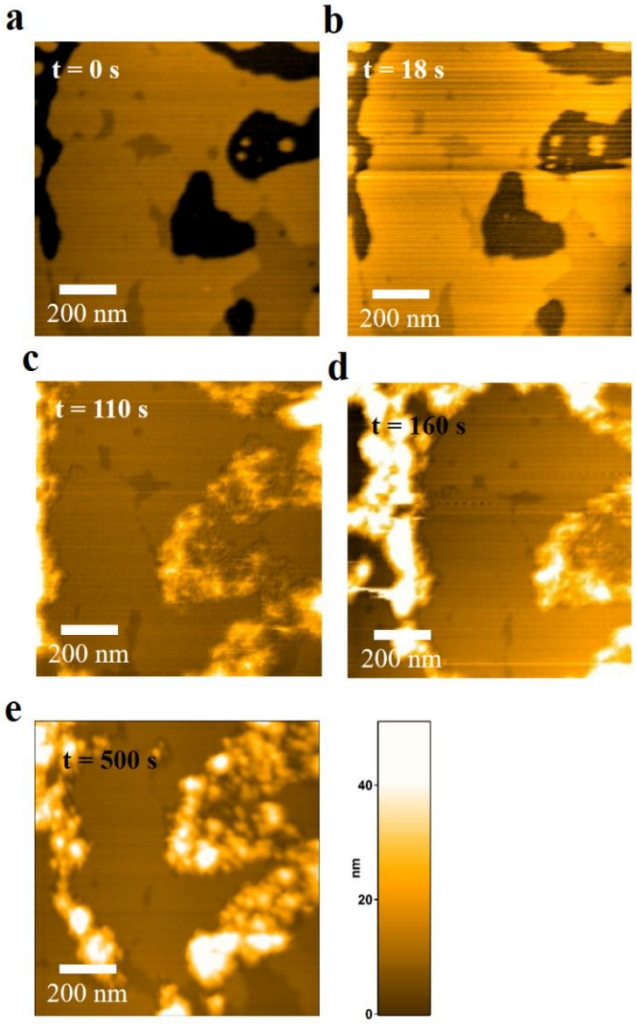

Figure 2: Interaction between $A\beta_{1-42}$oG37C peptide and a SM/DOPC biomimetic membrane. Successive HS-AFM images (a-e). Frame rate, 1s/frame; scan area, 800 × 800 nm² with 256 × 256 pixels². At t=18s, the peptide was injected in the fluid cell during imaging. Peptides are interacting only with the substrate while the membrane remains intact with time.

In a second step, a different lipid composition was assessed using biomimetic membrane composed of SM/POPC/Chol (20/60/20) to see the effect of the Cholesterol on the interactions. Once again, the scanned areas were selected to clearly distinguish both the mica substrate and the membrane surface. Snapshots extracted from the video (see video ESI4) showed that oG37C exhibited a behavior similar to the one observed on SM/POPC lipid layer, *i.e.* it spreads on the mica but almost not on the bilayer (Fig.3).

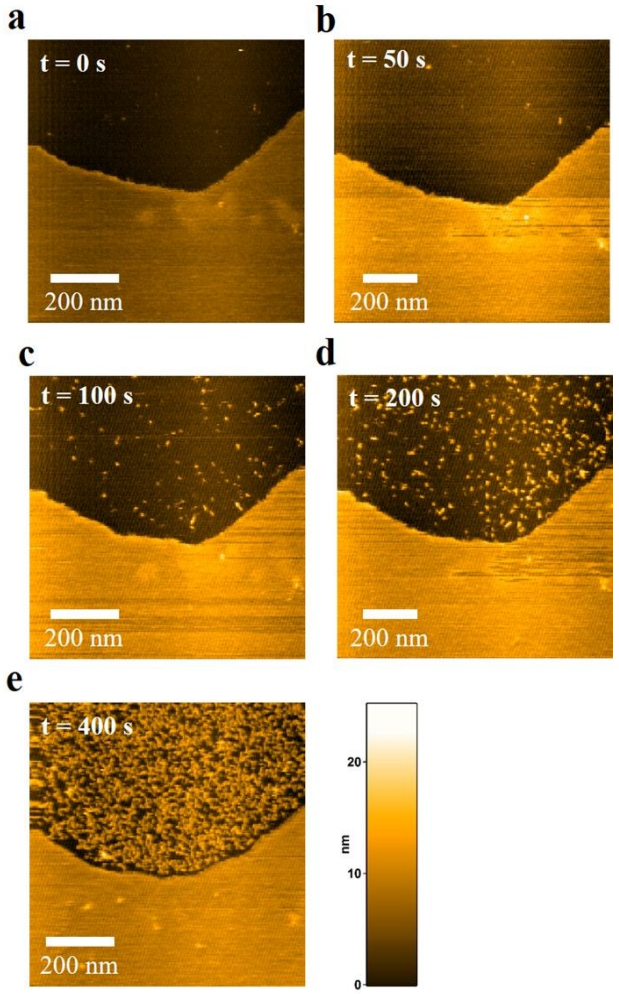

Figure 3: Interaction between $A\beta_{1-42}$ oG37C peptide and a SM/POPC/Chol biomimetic membrane. Successive HS-AFM images (a-e). Frame rate, 1s/frame; scan area, 800 × 800 nm² with 200 × 200 pixels². At t=42s, the peptide was injected in the fluid cell during imaging. No peptide was localized on the membrane, they just moved passively on the substrate.

In the figure 3 (but also in the figure 4 or ESI7 video for instance), some white spots could be seen on the membrane. Such spots are sometimes observed before injection on the membrane and on the mica and they should be due to some remaining membrane fragments in the solution, which deposit on the membrane with time. For most of these objects, their very low density, their sizes superior to the oligomer height and diameter, and their absence for most of the experiments are in favor of the fragment hypothesis even if we could not exclude that isolated

View Article Online
DOI: 10.1039/C8NR08714H

oG37C oligomers could be deposited on the membrane. Regarding the density of peptides on the substrate and even if some could be deposited on the membrane, their affinity for the substrate is more important than the one for the membrane.
After several tens of minutes, no disruptive effect was observed and the membrane remained intact with time. It can be concluded that oG37C does not interact preferentially with SM/POPC/Chol membrane and does not lead to a significant change of the membrane morphology. The presence of cholesterol by itself is not sufficient to induce a strong interaction between oG37C and membranes.

Interaction between $A\beta_{1-42}$ oG37C and SM/POPC/GM1 bilayer

Then, the impact of ganglioside GM1 on the interaction mechanism with the toxic oligomer oG37C was assessed using SM/POPC/GM1 (20/40/40) lipid membranes. Contrary to the two first conditions, after injection, the peptides clearly accumulated on both the lipid membrane and the mica as seen in Figure 4. Gradually, their density increased over time until a quasi-complete coverage was observed over the scanning area and beyond. The peptide diffusion could also be observed (see video ESI3 and ESI6) on the substrate and on the bilayers. As for the bare substrate, some peptides seem to have a fast diffusion (always in the same range of 38 nm²/s whatever the substrate or the membrane) while others are stuck on surface/membrane surface. However, no perturbation nor loss of the integrity of the lipidic membrane could be detected even after 15 minutes after injection. In contrast to the previous results obtained with SM/POPC and SM/POPC/Chol lipid layers, $A\beta_{1-42}$ oG37C accumulated on the surface of the lipid layer when ganglioside GM1 is present showing a better interaction between oG37C and the membrane linked to the presence of GM1.

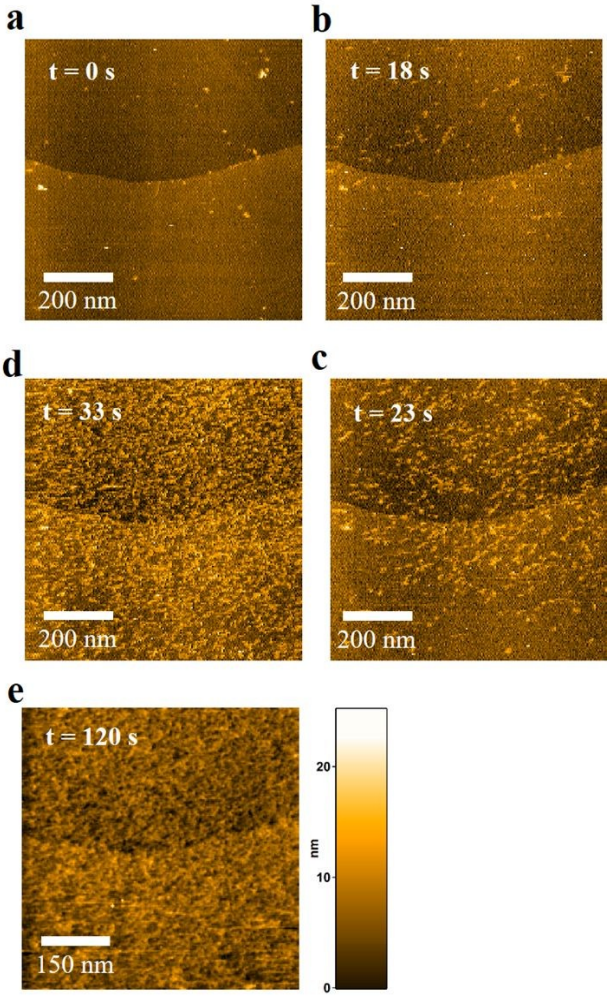

Figure 4: Interaction between $A\beta_{1-42}$ oG37C peptide and a SM/POPC/GM1 biomimetic membrane. Successive HS-AFM images (a-e). Frame rate, 1s/frame; scan area, 800 × 800 nm² with 200 × 200 pixels². At t=18s, the peptide is injected in the fluid cell during imaging.

Interaction between $A\beta_{1-42}$ oG37C and SM/POPC/GM1/Chol bilayer

The final step was to investigate the effect of these toxic oligomers oG37C on a more complex biomimetic membrane system containing SM, POPC, GM1 and Chol (20/20/40/20). Again, the scan area was focused on a region where membrane and mica substrate were clearly discernible, with some holes within the membranes. Contrary to the other compositions, a totally different behavior could be observed as a gradual disappearance of the membrane occurred after the injection of the toxic oligomer oG37C and in a very short time (Fig.5). The recorded video (ESI7) shows a complete dissolution of the

View Article Online
DOI: 10.1039/C8NR08714H

membrane occurring after 4 min of interaction after injection. Eventually, the interaction initiated a complete resorption/solubilization of the membrane system. Regarding the attack of the membrane by the peptides, it seems that it mostly begins at the edges of the membrane. When looking at ESI7 video and figure 5 where the membrane has some holes in it before the peptide injection, it seems that when the holes are too small, no clear evidence of membrane disruption starting at the edges of these holes could be observed, the disruption starting mostly at the long edges, as already observed in other studies related to membrane disruption[35]. To investigate further this point, the same experiment was performed but with a more continuous membrane. In video ESI8 and figure ESI9, the same disruption mechanism is observed but nevertheless, we could see a splitting of the membrane in two pieces which could indicate a disruption coming from the inside of the membrane in the same time as from the edges. This disruption process could then happen from both the edges and the inside of the membrane but with a faster rate when the length of the membrane edges is important which could prevent to follow the disruption coming from internal membranes parts. Even if some different behavior could be observed, the disruption of the membrane shown in videos ESI7 and ESI8 when its composition is SM/PC/Chol/GM1 is clearly due to the peptides as without oG37C, no change in the membrane integrity is observed over a long time (around 30 min) as seen in the ESI10 video. As HS-AFM allows a very high spatial resolution, no pore formation took place on the surface of the membrane, the oligomer seemed to anchor the edge of the lipid layer leading to its fast solubilization. The roughness analysis reveals the absence of any pores or defects on the membrane surface in this scan area.

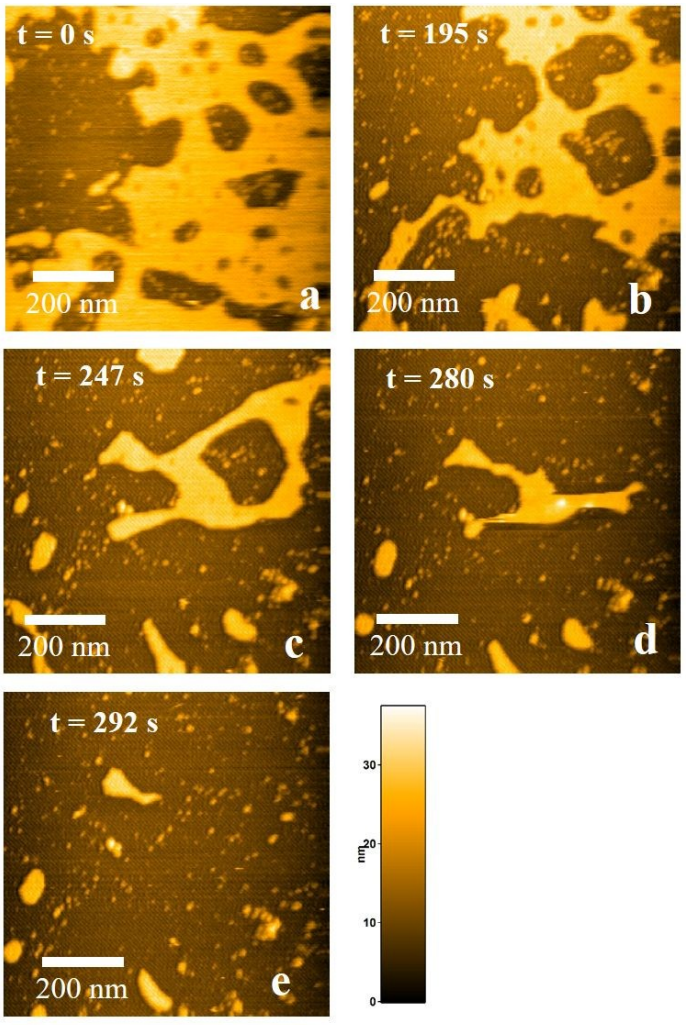

Figure 5: Interaction between $A\beta_{1-42}$ oG37C peptide and a SM/POPC/Chol/GM1 biomimetic membrane with holes. Successive HS-AFM images (a-j). Frame rate, 1s/frame; scan area, 800 × 800 nm² with 200 × 200 pixels². At t=80s, the peptide is injected in the fluid cell during imaging.

Regarding the peptides, contrary to previous conditions, no peptide is observed neither on the mica substrate (particularly on the ESI8 video) nor on the membranes. Such behavior is not obvious even if after disruption of the membranes of the figure 5, some remaining entities observed on the different images could be some small membrane pieces but also some peptides regarding their sizes. One hypothesis could be that because of an important affinity with the SM/PC/GM1/Chol membranes, when close to a membrane, the peptides are quickly diffusing on the membrane, which combined to a very fast insertion in the membrane does not enable to observe them at the speed of HS-AFM. Once the membrane is disrupted, as they were inserted within the membrane, because of their hydrophobic nature, they should strongly interact with the lipids torn from the membrane to form mixed oligomer/lipid micelles that remain in solution. The fact that we never observe oligomers on SM/POPC/GM1/Chol membranes is indeed surprising, but has been previously observed using classical AFM[35,36] or fast-scanning AFM[37] (10 sec/image) in similar systems. To further investigate this point, and even if the intrinsic speed of the setup limits the possible observations, another experiment was performed (video_ESI11 and fig. ESI12). First, a substrate area without any membrane was found and its position was recorded. Then, the AFM tip was displaced on another area with small membrane patches and the membrane morphology was followed upon peptide injection, confirming the membrane disruption as previously observed. At the end of the process, almost nothing could be observed on this area while when going back to the first recorded position initially empty, some rounded objects, similar in sizes and morphology to oG37C, are present on the substrate. This result is in line with our previous assumption suggesting that when close to a membrane of proper composition, the peptides are interacting with this membrane and could not be found on the mica substrate because of a fast diffusion process while far from a crowded membrane area before injection, peptides could interact with the substrate and could be found at the end at the process.

Another interesting point to investigate is the impact of the peptide concentration even if it is not obvious to have a precise quantification. Indeed, even if the peptides concentration were similar for each experiments, with the injection and the imaging processes inducing liquid perturbation in the area of the AFM tip

View Article Online
DOI: 10.1039/C8NR08714H

Lipidic composition of the membrane	Mechanisms	Results
SM/POPC	Peptides accumulated on the substrate.	No apparent interaction between oG37C and membrane. Membrane integrity preserved
SM/POPC/ Chol	Peptides accumulated on the substrate.	No apparent interaction between oG37C and membrane. Membrane integrity preserved.
SM/POPC/ GM1	Peptides accumulated on both substrate and lipid layer.	Interaction between oG37C and the membrane. Membrane integrity preserved.
SM/POPC/ GM1/Chol	Fast and total dissolution of the membrane.	Interaction between oG37C and membrane leading to a detergent effect.

Table 1: Overview of the interactions observed between the amyloid peptide $A\beta_{1-42}$ oG37C and different lipid membrane compositions

and the fact that we are investigating surface effect, it is quite difficult to have a precise and quantitative idea of their impact on the disruption. The most important parameter is not the concentration by itself but the local concentration of the peptides near the scanned area. This local concentration is not possible to be precisely controlled as many parameters, such as the influence of the tip movement, the distance between the syringe and the sample during the injection, the imaging parameters, or the membrane shape could change. For instance, with the exact same conditions, if we compare the videos from ESI 7 and 8, the disruption process is occurring in the two experiments but the time for total disappearance is different, from 80s to around 3 to 4min. This could be due to the difference in the membrane morphology (with holes or more continuous) or to the local concentration of the peptides. To see if a difference could be observed, an experiment using 5µM of peptide instead if 20µM was performed. As seen in video ESI13 and figure ESI14, for a membrane morphology similar to the one observed in figure 5, the same disruption mechanism is observed with a total time for the disappearance of the membrane around 5 to 6 min superior to the times evidenced for a peptide concentration of 20µM. Even if it is difficult to precisely control the local peptide concentration due to the perturbation of the tip, it obviously plays a role regarding the speed of the membrane disruption, the final effect is the same for the two experiments proving the importance of the membrane composition on its interaction with the peptides leading to its disruption.

$A\beta_{1-42}$ action on biomimetic neuronal membranes

To summarize, the experiments driven by HS-AFM described here showed the dynamic of interaction between the toxic amyloid peptide oG37C and model membranes of different composition. Indeed, among the different lipid compositions studied, distinct interaction mechanisms were highlighted in Table 1.

According to our results, GM1 is necessary for the toxic $A\beta_{1-42}$ oligomer oG37C to interact with the lipid layer. Indeed, it diffused not only on the substrate but also on the SM/POPC/GM1 membrane whereas it did not on the SM/POPC and the SM/POPC/Chol membranes. These results support the fact that the ganglioside GM1 would act as an anchor point for Aβ peptide which is in accordance with the mechanism of interaction proposed by Ikeda et al.[38]. Aβ binding to GM1 was also confirmed on living neuronal cells *in vitro*[39].

The results obtained with GM1/SM/PC lipid layer showed an affinity between Aβ and GM1, but this affinity is not sufficient to induce the destruction of the membrane. Experiments showed that in presence of Chol/SM/PC membrane, without GM1, cholesterol did not favor the interaction between Aβ and the membrane. The cooperative function of GM1 and cholesterol observed during our experiments has also been reported in other studies[40-42]. Indeed, it has been demonstrated that Aβ would be able to interact with GM1 only if those are gathered as clusters on the lipid layer[39,43]. As the involvement of cholesterol in the formation of lipid raft is now well-characterized, it is very likely that it would enhance GM1 clusterization[44]. It has been suggested that cholesterol would assist Aβ-GM1 interaction by facilitating conformational change of GM1 in order to increase its accessibility[42]. Cholesterol accelerates the interaction between Aβ and GM1 but does not impact the peptide affinity for the gangliosides, the interaction between Aβ and GM1 gangliosides is cholesterol dependent[42,45].

Furthermore, results showed a fast and total destruction of the membrane by the oligomer oG37C in around two to three minutes which seemed to be in accordance with the idea that oligomers are the interacting species (and not monomers or fibers). Indeed, Di Scala et al.[46] proposed that monomers would first insert into the membrane and undergo oligomerization through a cholesterol-regulated process. According to their study, Aβ would first insert in the membrane *via* cholesterol-rich domain and gangliosides would stabilize the intermediate species of the peptides, such as protofibrils and oligomers, through hydrogen bonds, charged groups and hydrophobic interaction with -CH groups of sugars[39]. Also, the complex formed by GM1 and $A\beta_{1-42}$ oG37C is suggested to act as a pattern that accelerates the formation of toxic oligomers and/or fibrils[47]. Aβ oligomers consequently formed have in turn, the capacity to interact with the GM1 present in the membrane[43]. Thus, GM1 would be involved in Aβ oligomer formation. This would explain the fast kinetic of membrane dissolution since oG37C peptides are already in an oligomeric state. Our results

View Article Online
DOI: 10.1039/C8NR08714H

are consistent with a study of Williams *et al* that demonstrate the toxicity of Aβ oligomers[48]. Furthermore, Nicastro et al.[49] reported the insertion of Aβ in GM1-cholesterol domains containing liposomes and highlighted the resulting structural perturbation into the internal layers of liposomes. Our observations are in accordance with this model since the interaction of oG37C with SM/POPC/Chol/GM1 membrane leads to the rupture of the membrane by a detergent effect. The results of the HS-AFM clearly show the importance of the membrane composition regarding the disruption process when interacting with toxic oligomeric oG37C. Even if the disruption seems to start from the edges of the membranes (or at least is faster when an edge with large size is available), such disruption could also happen in cells as during the biological process leading to interaction between peptides and membranes, some local forces could lead to differences in the membrane morphology that could be assimilated to an edge in our experiments.

To our knowledge, even though several studies have described the cooperation between cholesterol and GM1, this is the first time detergent effect of Aβ oligomers could be visualized with such a high temporal resolution and without having some competing effects coming from the peptide assembly process. Since the lipid composition of neuronal membranes is disturbed during the progression of AD or other physiological processes such as ageing, it is very important to understand how lipids could assist Aβ deleterious effect on neuronal cells. This work allowed us to propose an interaction mechanism (Fig. 6) between $A\beta_{1\text{-}42}$ amyloid peptides and membranes. Here we showed that Aβ, as oligomers, interact with GM1 clusters, present in membranes containing cholesterol leading to their solubilization.

$A\beta_{1-42}-G37C$	D A F R H D S G Y E V H H Q K L V F F A E D V G S N K G A I I G L H V **C** V V I A

Table 2: Amino-acid sequence of $A\beta_{1-42}$ oligomeric G37C (oG37C) mutant peptide

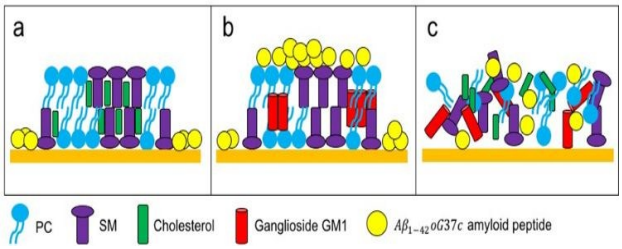

Figure 6: Schemes established from observations in order to describe the main interaction mechanisms. Depending on the composition of the membrane, peptides were observed only on the substrate (a), on the substrate and the membrane surface (b), or a fast dissolution of the whole system occurred (c).

Gangliosides GM1 act as an anchor point for the peptides and cholesterol is an essential element for membrane disruption. Regarding the peptides, amyloid peptides assemble from a monomer to form fibers. The toxic species are the so-called oligomeric intermediate forms. It is difficult to isolate these forms and to evaluate their effect on membranes. The oG37C is therefore a very good model for mimicking the impact of these species. In a recent study[50], we demonstrated that oG37C as well as wtAβ elicits its toxicity during its interaction with plasma membrane. The results are necessarily amplified here because in the *in vivo* process the concentration of oligomers must be much lower. Our results highlight the strong deleterious effects of oligomers on GM1-rich membranes.

Experimental

$A\beta_{1-42}$ peptides

The $A\beta_{1-42}$ variant oG37C (see table 2 for its primary structure) used in this study was selected in yeast, produced, and purified as previously described elsewhere[18,51]. Purity of the peptide was followed by size exclusion chromatography and by mass spectrometry. After purification, the oligomer $A\beta_{1-42}$ oG37C was pooled, frozen in liquid nitrogen, and conserved at −80 °C until use.

Lipid bilayers preparation

Materials.

1-Palmitoyl-2-oleoylphosphatidylcholine (POPC), sphingomyelin (SM), ganglioside GM1 (GM1) and cholesterol (>98 %) (Chol) were purchased from Avanti Polar Lipids, Inc. Ultrapure water with a nominal resistivity of 18 mΩ·cm (Milli-Q Millipore) was used for all buffers.

Liposome Preparation.

Liposome were prepared as described elsewhere[50]. Briefly, lipids were dissolved in chloroform/methanol (4:1 vol/vol) and mixed to the desired ratio (Table 3). The lipid solutions were evaporated under nitrogen flow and left under vacuum for 3–4 h to remove all organic solvent traces. The lipid films formed were hydrated with buffer (Tris-HCl 10 mM, NaCl 150mM, DTT 5mM, pH 7.4), vortexed and then subjected to five hot/cold cycles from liquid nitrogen to a 40 °C water bath before extrusion using membranes with pore diameter of 100 nm. The different compositions used are reported table 3.

Membrane model	SM (%)	PC (%)	GM1 (%)	Chol (%)
SM/POPC	20	80	×	×
SM/POPC/Chol	20	60	×	20
SM/POPC/GM1	20	40	40	×

View Article Online
DOI: 10.1039/C8NR08714H

SM/POPC/GM1/Chol	20	20	40	20

Table 3: Membrane model compositions used to observe the interaction with the peptide $A\beta_{1-42}$ oG37C. The percentages are (w/w) percentages.

High Speed Atomic Force Microscopy setup

A self-built high-speed atomic force microscope (HS-AFM) apparatus (Ando's model[52]) provided by RIBM was used. The cantilevers (Olympus) used were 6–7 µm long, 2 µm wide, and 90 nm thick. The spring constant was 0.1–0.2 N/m, and the resonant frequency and quality factor in an aqueous solution were 630 kHz and ~2, respectively. For HS-AFM imaging, the free oscillation amplitude was adjusted to ~2 nm, and the set-point amplitude was approximately 85% of the free oscillation amplitude. Tapping Mode was used for imaging and the loading force is kept with constant value. Specificity of HS-AFM (Ando's model) is that we are using a dynamic Proportionnal Integral Derivative controller for the feedback. In that sense, it can ensure and provide a technological duality of a low-invasiveness of the interaction tip-sample during imaging and simultaneously maintains an efficient bring-back contact of the tip to the sample even at high oscillation frequency, overcoming parachuting events[27].

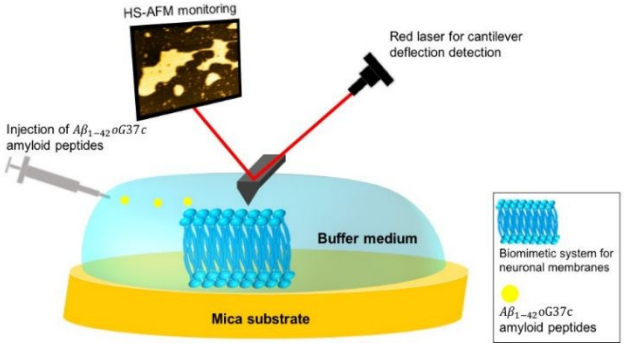

Figure 7: Operating setup for observation of interaction between $A\beta_{1-42}$ oG37C peptide and a biomimetic membrane. All the process occurring on the surface are recorded at the nanoscale, before, during and after injection of $A\beta_{1-42}$ oG37C.

An amorphous carbon tip was grown on the original tip through electron-beam deposition and then sharpened by plasma etching offering an apex of ~4-5 nm. For observations, a droplet of 2 µL of liposomes was deposited on a fresh cleaved mica, previously glued on a glass rod stage of 1.5 mm of diameter. After about 30 minutes of incubation, samples were rinsed with imaging buffer (Tris-HCl 10 mM, NaCl 150mM, DTT 5mM, pH 7.4). Peptide injection was realized during the observation. For the peptide, whatever the membrane composition, a volume of 6µl of the peptides at a concentration of 20µM was added to a volume of 74µL of buffer solution and then injected, except for the last experiments (Figure ESI14) for which 5µM of peptides were used instead of 20µM. The same volume of 80µL was injected into the liquid cell for each experiment while maintaining the tip scanning (Figure 7). The injection generates image jumps resulting of the difference of hydrodynamic pressure induced by the addition of solution in the liquid cell used for the experiments (see videos of the SI). To overcome that problem, the interaction force was adjusted simultaneously and a suitable value was ensured for the feedback monitoring the *x-y-z* direction of the piezoelectric scanner so that the images became stable again after few seconds. No alteration of the tip quality occurred since biomolecule resolution is provided on the videos recorded after injection and the scanned area remained similar than the one scanned before injection.

Each experimental condition was repeated at least three times and for each membrane, different places on the surface were scanned to ensure the consistency of the results. Results obtained between the replicates show a perfect reproducibility.
Diffusion coefficients were calculated after extracting successive images from raw data of HS-AFM videos with a self-built software working with Igor Pro (Wavemetrics). For each frame serie, (*x,y*) positions of a given amyloid peptide were recorded manually with the manual tracking plugin of ImageJ software. Amyloid peptide diffusion constant rates were calculated according to a Brownian diffusion model equation:
$D = \langle r^2 \rangle / 4t$ with $\langle r^2 \rangle$ the mean square displacement and t the time interval between each measured position.

Conclusions

In this study, High-Speed Atomic Force Microscopy was used to directly visualize at molecular scale and in real time the interaction mechanisms that occur between a toxic amyloid peptide variant, oG37C, and lipid layers of different compositions. The $A\beta_{1-42}$ oG37C peptide was chosen as a model for oligomeric structures thought to be responsible for Alzheimer's dementia onset and lipid bilayers were correspondingly used as biomimetic models for neuronal membranes. Our highly time-resolved data demonstrate how the association of cholesterol with ganglioside GM1 is essential for the destructive effect of the peptide following its interaction

View Article Online
DOI: 10.1039/C8NR08714H

with the lipid bilayer. Only the simultaneous presence of the two compounds allows to initiate the membrane dissolution since without one of those elements, no destruction occurred. Furthermore, the detergent effect involved could be visualized. Eventually, our results suggest a two-step mechanism: first the attachment and the accumulation of oG37C to GM1 domains of the membrane, then their insertion into the membrane via the cholesterol nearby, leading to a complete disruption of the membrane. If some questions are still raising regarding the diffusion speed of the peptides and the quantification of the affinities for the membranes regarding their compositions, the enormous potential of HS-AFM with recent new methodological developments[31,53] should enable in future studies to improve our knowledge of the different mechanisms involved in the peptide/membrane interactions.

Conflicts of interest

The authors report no conflicts of interest.

Author contributions

M.E., S.H., E.L.., C.F., M.M., and S.L. participated to the scientific discussions, analysed the data and wrote the manuscript. S.L. and M.M. designed the project and the methodology. M.E., E.L. and M.M. carried out the AFM experiments. S.H., M.E., C.F. and E.L. prepare the bilayers and the samples before AFM experiments. C.B. and C.C. prepared the oG37C peptides. M.M. and S.L. are the coordinators of the project. All authors read and approved the final manuscript.

Acknowledgements

The authors thank the FEDER, Région Grand Est and DRRT Grand Est for their support of the Nano'Mat platform and of the project through E. Lambert PhD's financial support. C. Feuillie has received funding from the European Union's Horizon 2020 programme under grant agreement No 794636.

Notes and references

1 T.L.W. Serpell, C. Louise, *FEBS J.,* 2011, **278**, 3905-3917.
2 L.N. Zhao, H. Long, Y. Mu, L.Y. Chew, *Int. J. Mol. Sci.*, 2012, **13**, 7303-7327.
3 A. Relini, O. Cavalleri, R. Rolandi, A. Gliozzi, *Chem. Phys. Lipids*, 2009, **158**, 1-9.
4 V. Koppaka, P.H. Axelsen, *Biochemistery*, 2000, **39**, 10011-10016.
5 T.A. Harroun, J.P. Bradshaw, R.H. Ashley, *FEBS Lett.*, 2001, **507**, 200-204.
6. F. Hane, E. Drolle, R. Gaikwad, E. Faught, Z. Leonenko, *J. Alzheimers Dis.*, 2011, **26**, 485–494
7 E. Drolle, A. Negoda, K. Hammond, E. Pavlov, Z. Leonenko, *PLoS ONE*, 2017, **12**, e0182194
8 H. Hayashi, N. Kimura, H. Yamaguchi, K. Hasegawa, T. Yokoseki, M. Shibata, N. Yamamoto, M. Michikawa, Y. Yoshikawa, K. Terao, *J. Neurosci.*, 2004, **24**, 4894–4902.
9 B. Wolozin, *Proc. Natl. Acad. Sci. USA*, 2001, **98**, 5371-5373.
10 J. Marx, Science, 2004, **294**, 508-509.
11 M. Bucciantini, S. Rigacci, M. Stefani, *J. Phys. Chem. Lett,*. 2014, **5,** 517-527.
12 N. Sanghera, B.E.F.S. Correia, J.R.S. Correia, C. Ludwig, S. Agarwal, H.K. Nakamura, K. Kuwata, E. Samain, A.C. Gill, B.B. Bonev, *Chem. Biol.*, 2011, **18**, 1422-1431.
13 V. Maglione, P. Marchi, A. Di Pardo, S. Lingrell, M. Horkey, E. Tidmarsh, S. Sipione, *J. Neurosci.*, 2010, **30**, 4072-4080.
14 K. Matsuzaki, K. Kato, K. Yanagisawa, *Biochim. Biophys. Acta.*, 2010, **1801**, 868-877.
15 K. Mori, M.I. Mahmood, S. Neya, K. Matsuzaki, T. Hoshino, *J. Phys. Chem. B.*, 2012, **116**, 5111-5121.
16 T. Valdes-Gonzalez, J. Inagawa, T. Ido, *Peptides*, 2001, **22**, 1099-1106.
17 Editorial, *Nature Neuroscience*, 2011, **14**, 399.
18 H. Vignaud, C. Bobo, I. Lascu, K.M. Sörgjerd, T. Zako, M. Maeda, B. Salin, S. Lecomte, C. Cullin, *PLoS ONE*, 2013, **8**, e80262.
19 M.O.W. Grimm, V.C. Zimmer, J. Lehmann, H.S. Grimm, T. Hartmann, T., *BioMed Research International,* 2013, **2013**, 814390.
20 F. D'Angelo, H. Vignaud, J. Di Martino, B. Salin, A. Devin, C. Cullin, C. Marchal, *Dis. Model. J. Mech.*, 2013, **6**, 206–216.
21 A. Choucair, M. Chakrapani, B. Chakravarthy, J. Katsaras, L.J. Johnston, *Biochim. Biophys. Acta*. 2007, **1768,** 146-154.
22 M.A. Sani, F. Separovic, J.D. Gehman, *Biophys. J.,* 2011, **100**, 40-42.
23 K. Sasahara, K. Morigaki, K. Shinya, *Phys. Chem. Chem. Phys.*, 2013, **15**, 8929-8939.
24 L. Fu, Z. Wang, V.S. Batista, E.C.Y. Yan, *J. Diabetes Res.*, 2016, **2016**, 1-17.
25 F. Hane, E. Drolle, R. Gaikwad, E. Faught, Z. Leonenko, J. Alzheimers Dis., 2011, **26**, 485-494.
26 E. Drolle, F. Hane, B. Lee, Z. Leonenko, *Drug. Metab. Review*, 2014, **46**, 207-223.
27 T. Ando, T. Uchihashi, S. Scheuring, *Chem. Rev.,* 2014, **114**, 3120-3188.
28 S. Bonhommeau,D. Talaga, J. Hunel, C. Cullin, S. Lecomte, *Angew. Chem. Int. Ed.*, 2017, **56**, 1771-1774.
29 C. Bobo, S. Chaignepain, S.Henry, H. Vignaud, A. Améadan, C.Marchal, E.Prado, J. Doutch, J.-M. Schmitter, C. Nardin, S. Lecomte, C. Cullin, *Biochim. Biophys. Acta* A, 2017, 1861, 1168-1176.
30 I. Casuso, P. Sens, F. Rico, S. Scheuring, *Biophys. J.*, 2010, **99**, L47–L49
31 R. Heath, S. Scheuring, Nat. Commun., 2018, 9, 4983

View Article Online
DOI: 10.1039/C8NR08714H

32 B. Onoa, S. Fukuda, M. Iwai, K.K. Niyogi, C. Bustamante, *Biophys. J.*, 2018, **114**, 70A

33 J.E. Shaw, R.F. Epand, J.C.Y. Hsu, G.C.H. Mo, R.M. Epand, C.M. Yip, *J. Struct. Biol.*, 2008, **162**, 121–138

34 M. Staykova, D.P. Holmes, C. Read, H.A. Stone, *Proc. Natl. Acad. Sci. USA*, 2011, 108, **22**, 9084-9088

35 K. El Kirat, V. Duprès, Y.F. Dufrêne, *Biochim. Biophys. Acta*, 2008, **1778**, 276–282

36 J. Pan, P.K. Sahoo, A. Dalzini, Z. Hayati, C.M. Aryal, P. Teng, J. Cai , H. Rodriguez Gutierrez, L. Song, *J. Phys. Chem. B*, 2017, **121**, 5058−5071

37 G.R. Heath, P.L. Harrison, P.N. Strong, S.D. Evans, K. Miller, *Soft Matter*, 2018, **14**, 6146

38 K. Ikeda, T. Yamaguchi, S. Fukunago, M. Hoshino, K. Matsuzaki, *Biochemistry* 2011, **50**, 6433-6440.

39 A. Kakio, S. Nishimoto, K. Yanagisawa, Y. Kozutsumi, K. Matsuzaki, *J. Biol. Chem.*, 2001, **276**, 24985-2499.

40 K. Yanagisawa, *BBA Biomembrane*, 2007, **1768**, 1943–1951.

41 M.C. Nicastro, D. Spigolon, F. Librizzi, O. Moran, M.G. Ortore, D. Bulone, P.L. San Biagio, R. Carrotta,. *Biophys. Chem.,* 2015, **208**, 9-16.

42 J. Fantini, N. Yahi, N. Garmy, *Front. Physiol.*, 2013, **4**, 120.

43 M. Calamai, F.S. Pavone, *FEBS Lett.*, 2013, **587**, 1385-1391.

44 M. Wakabayashi, T. Okada, Y. Kozutsumi K. Matsuzaki, *Biochem, Biophys. Res. Commun*., 2005, **328**, 1019–1023.

45 M. Manna, C. Mukhopadhyay, *PLoS ONE*, 2013, **8(8)**: e71308.

46 C. Di Scala, H. Chahinian, N. Yahi, N. Garmy, J. Fantini, *Biochemistry*, 2014, **53**, 4489−4502.

47 N. Yamamoto, E. Mastubara, S. Maeda, H. Minagawa, A. Takashima, W. Maruyama, M. Michikawa, K. Yanagisawa, *J. Biol. Chem.*, 2007, **282**, 2646-2655.

48 T.L. Williams, I.J. Day, L.C. Serpell, *Langmuir*, 2010, **26** (22), 17260-17268.

49 L. Caillon, L. Duma, O. Lequin, L. hemtemourian, *Mol. Membr. Biol.,* 2014, **31**, 239-249.6

50 G. Fruhmann, C. Marchal, H. Vignaud, M. Verduyckt, N. Talarek, C. De Virgilio, J. Winderickx, C. Cullin, *Front. Mol. Neurosci.,* 2018*,* **11**, 406.

51 S. Henry, H. Vignaud, C. Bobo, M. Decossas, O. Lambert, E. Harte, I.D. Alves, C. Cullin, S. Lecomte, *Biomacromolecules,* 2015, **16**, 944-950.

52 T. Ando, N. Kodera, E. Takai, D. Maruyama, K. Saito, A. Toda, *Proc. Natl. Acad. Sci. USA*, 2001, **98**, 12468-12472.

53 T. Mori, S. Sugiyama, M. Byrne, C. Hirschie Johnson, T. Uchihashi, T. Ando,, *Nat. Commun.*, 2018, **9**, 3245